



Continuous-variable entanglement swapping with photon subtractionNa Wang, Meihong Wang, and Xiaolong Su ^{*}*State Key Laboratory of Quantum Optics and Quantum Optics Devices, Institute of Opto-Electronics, Shanxi University, Taiyuan, 030006, China*
and Collaborative Innovation Center of Extreme Optics, Shanxi University, Taiyuan, Shanxi 030006, China (Received 16 November 2023; revised 9 April 2024; accepted 17 June 2024; published 3 July 2024)

Entanglement swapping, which establishes entanglement between two independent and distant entangled states, is a key element of a quantum repeater in an entanglement-based quantum network. In continuous-variable (CV) entanglement swapping, it is essential to enhance the entanglement of entanglement swapping because it decreases with loss and noise in the quantum channel. Here, we propose a scheme of enhancing entanglement of CV entanglement swapping by a photon subtraction (PS) operation in noisy channels. We apply both one- and two-sided PS operations in CV entanglement swapping through lossy single- and dual-channel transmission schemes, respectively. In the lossy channel, we show that the two-sided PS operation enables one to obtain higher entanglement and longer transmission distance compared to the one-sided PS operation. Furthermore, we show that the two-sided PS operation can enhance the entanglement of the entanglement swapping in the noisy single-channel CV entanglement swapping. Our results provide a feasible solution to enhance entanglement of CV entanglement swapping, and they have potential applications in building quantum repeaters.

DOI: [10.1103/PhysRevA.110.012416](https://doi.org/10.1103/PhysRevA.110.012416)**I. INTRODUCTION**

Quantum repeaters play an important role in long-distance quantum communication among distant quantum nodes. To build a quantum repeater in the entanglement-based quantum network, it is necessary and essential to realize entanglement swapping, which establishes entanglement between two independent and distant entangled states [1–4]. As one mode of an entangled state is teleported in entanglement swapping, it is also known as quantum teleportation of the entangled state [2–4]. Since the first experimental demonstration of entanglement swapping in the discrete-variable (DV) optical system [5], it is also demonstrated in the continuous-variable (CV) [6–8] and hybrid CV-DV [9,10] systems, respectively.

The most experimental demonstrations of entanglement swapping are limited to the proof-of-principle experiment, where the effect of loss and noise in the quantum channel is not considered. Towards practical application, it is essential to consider the effect of loss and noise in quantum channels since they lead to decoherence of quantum entanglement [11], even the sudden death of it [12,13]. In the CV entanglement swapping through the fiber channel, the output entanglement decreases inevitably since the fiber channel introduces loss and excess noise, which limits the application of entanglement after the swapping. Therefore, it is necessary and essential to enhance the entanglement of the CV entanglement swapping in a noisy channel.

For the CV entanglement, it has been shown that Gaussian states cannot be distilled with Gaussian operations [14–16]. To distill or enhance the Gaussian entanglement,

non-Gaussian operations are necessary, such as photon subtraction (PS) [17–21], photon addition (PA) [19,22,23], and photon replacement [24–26]. These non-Gaussian operations have been applied to enhance the performance of quantum teleportation [27–29], quantum key distribution [30–32], and quantum metrology [33–35]. In these presented schemes with non-Gaussian operations, the CV quantum resource (Gaussian states) is combined with the DV measurement technique (photon detection), which is a typical hybrid CV-DV quantum information processing [36–38]. Recently, non-Gaussian entanglement swapping has also been proposed, where non-Gaussian states are employed as the entanglement resource [39]. In the previous investigations, non-Gaussian operations are applied to enhance the entanglement of the two-mode Gaussian entangled state directly, while it remains unclear whether the non-Gaussian operations can enhance the entanglement of CV entanglement swapping.

In this paper, we propose a scheme for enhancing entanglement of CV entanglement swapping by PS operations in noisy channels. At first, we apply the one- and two-sided PS operations to CV entanglement swapping between two CV Einstein-Podolsky-Rosen (EPR) states without transmission in the quantum channel, respectively. By calculating the logarithmic negativity, which is used to quantify the entanglement before and after the PS operations, we show that the entanglement of CV entanglement swapping without loss is enhanced by both one- and two-sided PS operations in a certain squeezing range. Secondly, we apply one- and two-sided PS operations to CV entanglement swapping in both the lossy single- and dual-channel transmission schemes. The results show that the two-sided PS operation enables one to obtain higher entanglement and longer transmission distance compared to the one-sided PS operation. The maximum

^{*}Contact author: suxl@sxu.edu.cn

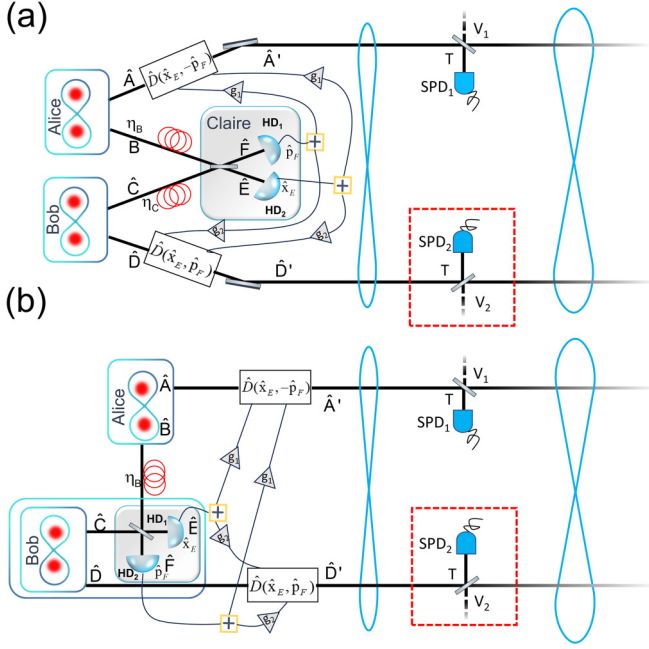


FIG. 1. The schemes for enhancing entanglement of CV entanglement swapping by PS operations in the (a) dual channel and (b) single channel. The one-sided PS is performed if there is no red dashed box. HD: homodyne detector, SPD: single photon detector, \boxplus : power splitter.

transmission distance for the single-channel transmission scheme is longer than that of the dual-channel transmission scheme. Thirdly, in a noisy single channel, we show that the two-sided PS operation can enhance the entanglement of CV entanglement swapping, and the maximum transmission distances where the two-sided PS operation takes effect decrease with the increase of excess noise. The presented results have potential applications in building quantum repeaters with CV entanglement.

II. THE SCHEME

The principle of the proposed scheme is shown in Fig. 1. In the CV entanglement swapping, Alice and Bob own two space-separated CV EPR entangled states with modes (\hat{A}, \hat{B}) and (\hat{C}, \hat{D}) , respectively. We consider two kinds of transmission schemes, namely dual- and single-channel schemes, respectively, as shown in Figs. 1(a) and 1(b). In the dual-channel transmission scheme [Fig. 1(a)], Alice and Bob send one of their EPR entangled states (modes \hat{B} and \hat{C}) to a third party, Claire, through quantum channels with transmission efficiencies η_B and η_C , respectively. Claire performs the joint measurement on modes \hat{B} and \hat{C} by coupling them on a 1:1 beam splitter. The output modes \hat{E} and \hat{F} are measured by two homodyne detectors (HD₁, HD₂), respectively. The measurement results of joint measurement are fed forward to modes \hat{A} and \hat{D} via classical channels. Alice and Bob displace the modes \hat{A} and \hat{D} according to the received measurement results. Finally, entanglement is established between distant modes \hat{A}' and \hat{D}' . In the single-channel transmission scheme [Fig. 1(b)], Alice transmits the mode \hat{B} to Bob through a quantum channel with transmission efficiency η_B . In this case, Bob implements

the joint measurement on the received mode \hat{B} and his own mode \hat{C} , and feeds forward the measurement results to modes \hat{A} and \hat{D} . To enhance the entanglement of entanglement swapping, the one- or two-sided PS operations are considered. In the two-sided PS, modes \hat{A}' and \hat{D}' are mixed with two vacuum states (V_1 and V_2) on the beam splitters with transmittances T , which reflects a small fraction of light to the single photon detectors SPD₁ and SPD₂, respectively. The click of both detectors indicates the success of the two-sided PS operation. In the one-sided PS, the PS is only applied to the mode \hat{A}' , and the click of SPD₁ indicates the success of the one-sided PS operation.

In the CV quantum information processing, the information is encoded in the amplitude and phase quadratures of photonics harmonic oscillators [40], which are expressed by $\hat{x} = \hat{a} + \hat{a}^\dagger$ and $\hat{p} = (\hat{a} - \hat{a}^\dagger)/i$, respectively. In this case, variances of amplitude and phase quadratures for a vacuum state are $V_{\hat{x}_0} = V_{\hat{p}_0} = V_0 = 1$, in which the subscript 0 represents a vacuum state. A Gaussian entangled state can be characterized by its covariance matrix

$$\sigma_{AB} = \begin{pmatrix} \sigma_A & \gamma_{AB} \\ \gamma_{AB}^\top & \sigma_B \end{pmatrix} = \begin{pmatrix} a & 0 & c_1 & 0 \\ 0 & a & 0 & c_2 \\ c_1 & 0 & b & 0 \\ 0 & c_2 & 0 & b \end{pmatrix}, \quad (1)$$

where the submatrices σ_A and σ_B are diagonal blocks of reduced states of subsystems, and γ_{AB} and γ_{AB}^\top are the off-diagonal matrices of intermodal correlations between subsystems. When the submodes \hat{A} and \hat{B} pass through noisy channels, the elements of the covariance matrix are given by

$$a = \eta_A \cosh 2r + (1 - \eta_A)(V_0 + \delta_A), \quad (2)$$

$$b = \eta_B \cosh 2r + (1 - \eta_B)(V_0 + \delta_B), \quad (3)$$

$$c_1 = -\sqrt{\eta_A \eta_B} \sinh 2r, \quad (4)$$

$$c_2 = \sqrt{\eta_A \eta_B} \sinh 2r, \quad (5)$$

where η_A and η_B are the transmission efficiencies of modes \hat{A} and \hat{B} , and δ_A and δ_B are the excess noise of modes \hat{A} and \hat{B} . The quantum channel is a lossy or noisy channel when $\delta_A = \delta_B = 0$ or $\delta_A = \delta_B > 0$. The same definition applies for the covariance matrix σ_{CD} of the CV entangled state with modes \hat{C} and \hat{D} ; the corresponding transmission efficiencies and excess noises are η_C (η_D) and δ_C (δ_D), respectively.

To realize CV entanglement swapping, joint measurement is implemented between modes \hat{B} and \hat{C} , which are coupled on a 1:1 beam splitter, and the output modes are $\hat{E} = (\hat{B} - \hat{C})/\sqrt{2}$ and $\hat{F} = (\hat{B} + \hat{C})/\sqrt{2}$. The amplitude and phase quadratures of the optical modes \hat{E} and \hat{F} , which are $\hat{x}_E = (\hat{x}_B - \hat{x}_C)/\sqrt{2}$ and $\hat{p}_F = (\hat{p}_B + \hat{p}_C)/\sqrt{2}$, are measured by two homodyne detectors, respectively. Then the measurement results of $\hat{x}_E = \hat{x}_E/2$ and $\hat{p}_F = \hat{p}_F/2$, which are obtained by splitting the measurement results of \hat{x}_E and \hat{p}_F with the power splitter (\boxplus), are fed forward to the optical mode \hat{A} with gain g_1 through the classical channels, while the other half of the measurement results are fed forward to the mode \hat{D} with gain g_2 . The optical modes \hat{A} and \hat{D} are displaced according to the

TABLE I. The optimal gains and logarithmic negativity for the single-channel entanglement swapping at different transmission distances.

Distance (km)	g_1	g_2	Logarithmic negativity
2	0.354	0.366	0.835
4	0.345	0.368	0.725
6	0.335	0.371	0.634
8	0.326	0.374	0.55
10	0.317	0.377	0.483
12	0.307	0.379	0.424
14	0.297	0.381	0.375
16	0.288	0.385	0.332
18	0.279	0.387	0.294
20	0.27	0.389	0.262
22	0.261	0.392	0.234
24	0.251	0.394	0.207
26	0.243	0.397	0.186
28	0.234	0.399	0.168
30	0.225	0.401	0.141

measurement results. The optical modes of the output state after entanglement swapping are [41]

$$\hat{A}' = \hat{A} + 2g_1\tilde{x}'_E - i2g_1\tilde{p}'_F, \quad (6)$$

$$\hat{D}' = \hat{D} + 2g_2\tilde{x}'_E + i2g_2\tilde{p}'_F, \quad (7)$$

where $g_1 = g_2 = \sinh 4r/4$ with $\eta_A (\eta_B) = \eta_C (\eta_D) = 1$ [42]. The covariance matrix of the output state is given by

$$\sigma_{A'D'} = \begin{pmatrix} a' & 0 & c'_1 & 0 \\ 0 & a' & 0 & c'_2 \\ c'_1 & 0 & d' & 0 \\ 0 & c'_2 & 0 & d' \end{pmatrix}, \quad (8)$$

where $a' = d' = [3 + \cosh(4r)] \operatorname{sech}(2r)$, $c'_2 = -c'_1 = \sinh(2r) \tanh(2r)$. And the covariance matrices $\sigma_{A'D'}$ at each transmission distance and excess noises can be obtained by choosing the gains according to Table I–IV, respectively. The gains are chosen by maximizing the entanglement after the entanglement swapping.

Since the quantum state becomes a non-Gaussian state after the PS operations, it is necessary to choose an entanglement quantity that can quantify both the Gaussian entangled state and the non-Gaussian state. Here, we choose the log-

TABLE II. The optimal gains and logarithmic negativity for the dual-channel entanglement swapping at different transmission distances.

Total distance (km)	g_1	g_2	Logarithmic negativity
4	0.356	0.356	0.709
8	0.349	0.349	0.509
12	0.342	0.342	0.332
16	0.359	0.334	0.215
18	0.326	0.326	0.237
20	0.317	0.317	0.149

TABLE III. The optimal gains and logarithmic negativity for the noisy single-channel entanglement swapping with the excess noise $\delta_B = 0.2$ SNU at different transmission distances.

Distance (km)	g_1	g_2	Logarithmic negativity
2	0.350	0.364	0.810
4	0.338	0.365	0.685
6	0.327	0.367	0.583
8	0.314	0.368	0.492
10	0.304	0.370	0.420
12	0.293	0.372	0.361
14	0.281	0.373	0.312
16	0.271	0.374	0.264
18	0.260	0.376	0.228
20	0.251	0.377	0.190
22	0.241	0.379	0.161

arithmic negativity, which is a computable measure of the entanglement and can be calculated under the Fock basis to quantify the entanglement before and after the PS operations. The logarithmic negativity is given by [43,44]

$$E_N(\rho) = \log_2[1 + 2N(\rho)], \quad (9)$$

where $N(\rho)$ is the absolute value of the sum of negative eigenvalues of the partially transposed density operator.

To obtain the logarithmic negativity, the density matrix is calculated. For calculating the density matrix, first the covariance matrix is transformed to its Wigner function via [40]

$$W_{A'D'} = \frac{1}{\sqrt{\operatorname{Det} \sigma_{A'D'} \pi^2}} \exp \left\{ -\frac{1}{2} (\xi^\top \sigma_{A'D'}^{-1} \xi) \right\}. \quad (10)$$

Second, the density matrix $\hat{\rho}_{A'D'}$ is obtained by calculating its elements according to the corresponding Wigner function. The elements of the two-mode density matrix are given by [45]

$$\rho_{klmn} = 16\pi\sigma_0^2 \iiint W_{A'D'} W_{|k\rangle\langle l|}(x_{A'}, p_{A'}) \times W_{|m\rangle\langle n|}(x_{D'}, p_{D'}) dx_{A'} dp_{A'} dx_{D'} dp_{D'}, \quad (11)$$

where

$$W_{|k\rangle\langle l|}(x, p) = \frac{(-1)^l}{2\pi\sigma_0^2} \sqrt{\frac{l!}{k!}} \left(\frac{x - ip}{\sigma_0} \right)^{k-l} \times e^{-(x^2 + p^2)/2\sigma_0^2} L_l^{k-l} \left(\frac{x^2 + p^2}{\sigma_0^2} \right). \quad (12)$$

TABLE IV. The optimal gains and logarithmic negativity for the noisy single-channel entanglement swapping with $\delta_B = 5$ SNU at different transmission distances.

Distance (km)	g_1	g_2	Logarithmic negativity
1	0.319	0.351	0.628
2	0.281	0.339	0.405
3	0.250	0.331	0.285
4	0.222	0.322	0.179
5	0.199	0.314	0.117

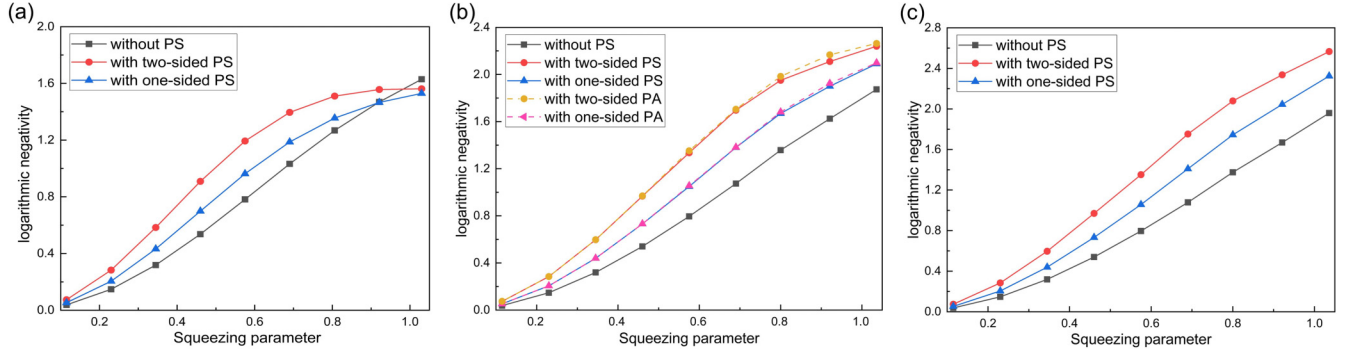


FIG. 2. The dependence of entanglement of CV entanglement swapping with and without PS or PA operation on the squeezing parameter for different truncations. (a) $N = 4$, (b) $N = 6$, (c) $N = 8$. The transmittance of the beam splitter in the PS and PA operations is chosen as $T = 0.99$.

In our calculation, the calculated density matrices $\hat{\rho}_{A'D'}$ are truncated to the photon number $N = 6$.

The PS operation is simulated by a beam splitter with transmittance $T = 0.99$ and a single photon detector with operators $\hat{\Pi}^{(\text{off})} = |0\rangle\langle 0|$ and $\hat{\Pi}^{(\text{on})} = 1 - \hat{\Pi}^{(\text{off})} = \sum_{k=1}^{\infty} |k\rangle\langle k|$, where $\hat{\Pi}^{(\text{off})}$ indicates no photon is detected and $\hat{\Pi}^{(\text{on})}$ represents at least one photon is detected [18]. The obtained density matrix is mixed with two vacuum states (V_1 and V_2) on the beam splitters with transmittance T to obtain $\hat{\rho}_{A'D'V_1V_2}$. One-sided PS operation means the projection of $\hat{\rho}_{A'D'V_1V_2}$ to the operator $I_{A'D'} \otimes (|0\rangle_{V_1}\langle 0|) \otimes (I - |0\rangle_{V_2}\langle 0|)$, while two-sided PS operation means that of $I_{A'D'} \otimes (I - |0\rangle_{V_1}\langle 0|) \otimes (I - |0\rangle_{V_2}\langle 0|)$. The density matrix after the PS operation $\hat{\rho}_{A'D'}^{\text{sub}}$ can be obtained by tracing out the vacuum modes V_1 and V_2 . To quantify the entanglement of the entanglement swapping before and after the PS operation, we calculate logarithmic negativity according to the obtained $\hat{\rho}_{A'D'}$ and $\hat{\rho}_{A'D'}^{\text{sub}}$.

III. RESULTS AND DISCUSSION

At first, the quantum channel without loss is considered. The dependences of logarithmic negativity for the one- and two-sided PS operations on the squeezing parameter of the CV entangled state with different truncation $N = 4, 6, 8$ of the calculated density matrices are shown in Figs. 2(a)–2(c), respectively. Comparing Figs. 2(a)–2(c), we show that the logarithmic negativity increases and the enhancement of entanglement by non-Gaussian operations is more obvious, especially for the relatively higher squeezing parameter, with the increase of the truncation number. This is because the CV entangled state with higher squeezing parameter involves more photon numbers. Since the results of the enhancement of CV entanglement swapping with PS operations at different truncations $N = 4, 6, 8$ present the same tendencies, and the logarithmic negativity of the one-sided PS and two-sided PS with $N = 6$ is only lower than that with $N = 8$ for 0.17% and 0.25%, respectively, in the case of $r = 0.46$, we choose $N = 6$ and $r = 0.46$ in our calculations by considering the tradeoff between computational complexity and precision.

In Fig. 2, compared to the logarithmic negativity of the entangled state without PS operations, both one- and two-sided PS operations can enhance the entanglement of entanglement swapping, and we show that the enhancement of entangle-

ment with a two-sided PS operation is higher than that of a one-sided PS operation. In addition to PS operation, PA operation is another type of typical non-Gaussian operation. In Fig. 2(b), we show the dependencies of logarithmic negativities on the squeezing parameter with one- and two-sided PA operations. We show that the enhancement of entanglement with two-sided PA operation is higher than that of one-sided PA operation. Compared to the results of PS operations, PA operation enables one to obtain higher logarithmic negativity in the range of relatively higher squeezing parameters ($r > 0.69$), while PA and PS operations enhance the logarithmic negativity with the same amount in the range of lower squeezing parameters ($r \leq 0.69$). Photon subtraction operation, which is realized by a beam splitter with low reflectivity and a single photon detector, has been widely demonstrated experimentally as a mature technique, such as in the preparation of non-Gaussian states and the distillation of Gaussian entangled states [46–52]. For photon addition and replacement operations, an additional source of single-photon state that has the same frequency as the entangled state is required [53]. These are more difficult in the experimental demonstration compared to the photon subtraction operation. Considering the experimental feasibility of three non-Gaussian operations, we focus on the PS operation in the following analysis.

The dependences of logarithmic negativity and success probability on the transmittance of the beam splitter for PS operations are presented in Fig. 3. PS operations can only enhance the entanglement after the entanglement swapping when the transmittance exceed a certain value. For example, as shown in Fig. 3(a), PS operations can enhance the entanglement when transmittances are higher than 0.72 and 0.82 for $r = 0.345$ and 0.8, respectively. We show that the logarithmic negativity increases with the increase of the transmittance of photon subtraction. $T = 0.99$ is chosen in our calculations to obtain relatively higher logarithmic negativity at the expense of low success probability, as shown in Fig. 3(b).

Secondly, we consider the enhancement of entanglement of CV entanglement swapping in lossy channels. The logarithmic negativity with and without one- and two-sided PS operations in the lossy single- and dual-channel transmission schemes is shown in Figs. 4(a) and 4(b), respectively. The results show that the entanglement with the two-sided PS operation is obviously higher than that with the one-sided

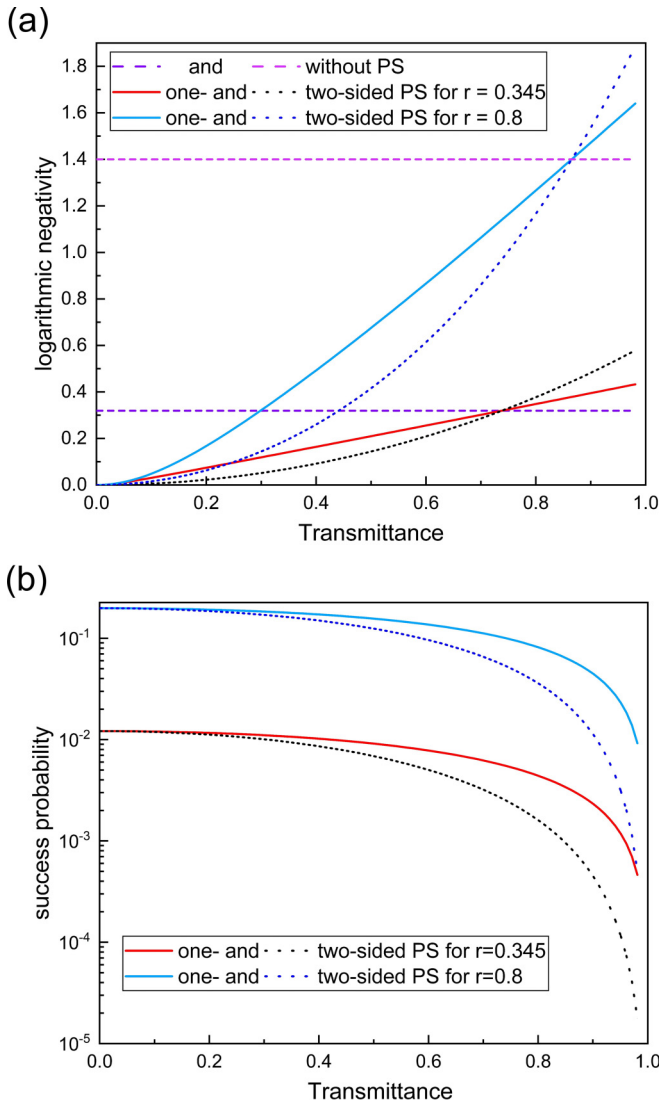


FIG. 3. (a) The dependences of logarithmic negativity on the transmittance of a beam splitter for PS operations. The upper blue solid and blue dotted lines represent the dependences of logarithmic negativity on the transmittance for $r = 0.8$, while the lower red solid and black dotted lines represent those for $r = 0.345$. The upper pink dashed and lower purple dashed lines are logarithmic negativities for $r = 0.8$ and 0.345 without PS operation, respectively. (b) The dependences of success probability on the transmittance of the beam splitter for PS operations. The upper blue solid and blue dotted lines represent the dependences of success probability on the transmittance for $r = 0.8$, while the lower red solid and black dotted lines represent those for $r = 0.345$.

PS operation in this case, where the squeezing parameter $r = 0.46$ (corresponding to 4 dB squeezing), transmission loss of $\alpha = 0.2$ dB/km in the fiber channel, and optimal gains in Tables I and II are chosen. As shown in Fig. 3(a), in the single-channel transmission scheme of entanglement swapping, the two-sided PS operation can enhance the entanglement in the range of $0 < L < 30$ km, while only a small extent of transmission distance ($0 < L < 1.9$ km) does so for the one-sided PS operation. In the dual-channel transmission scheme of CV entanglement swapping, the total transmission distance is the

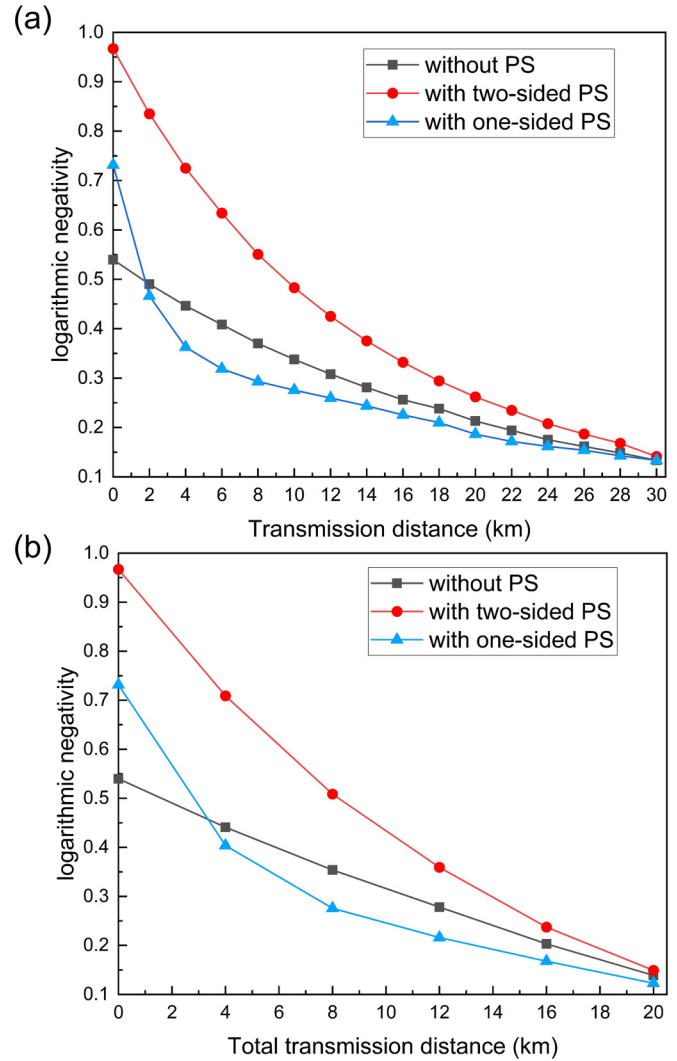


FIG. 4. The dependences of logarithmic negativity on the transmission distance for one- and two-sided PS operations in the (a) single- and (b) dual-channel entanglement swapping schemes with parameters $r = 0.46$ and $T = 0.99$.

sum of the transmission distances in two quantum channels, where the transmission efficiencies in two quantum channels are chosen to be equal ($\eta_B = \eta_C$) for simplification. As shown in Fig. 3(b), we show that the two-sided PS operation can enhance the entanglement in the range of $0 < L < 20$ km while only a small extent of transmission distance ($0 < L < 3.5$ km) does so for the one-sided PS operation in the dual-channel entanglement swapping. Comparing the results in Figs. 3(a) and 3(b), we show that the maximum transmission distance at which the entanglement can be enhanced by the two-sided PS operation in the single-channel transmission scheme is longer than that in the dual-channel transmission scheme.

Finally, we consider the enhancement of entanglement in the single-channel CV entanglement swapping with two-sided PS operation since it enables one to obtain higher entanglement based on the above results. The dependence of logarithmic negativity on the transmission distances in the noisy single channel is shown in Fig. 5. We show that the enhancement of entanglement is obtained in the range of

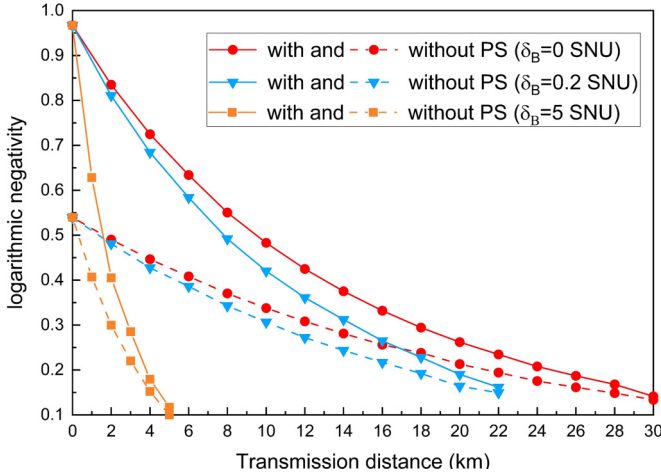


FIG. 5. The dependences of logarithmic negativity on the transmission distance in a noisy single-channel scheme for different excess noise with parameters $r = 0.46$ and $T = 0.99$. The excess noise is taken as $\delta_B = 0, 0.2,$ and 5 SNU for comparison.

$0 < L < 30, 0 < L < 22,$ and $0 < L < 5$ km when the excess noise in the quantum channel is $0, 0.2,$ and 5 shot-noise unit (SNU), respectively, where the squeezing parameter $r = 0.46$ (corresponding to 4 dB squeezing) and optimal gains in Tables I, III, and IV are chosen. Comparing the results with different excess noises, we demonstrate that the maximum transmission distances at which the two-sided PS operation takes effect decrease with the increase of excess noise in the noisy single-channel scheme.

IV. CONCLUSION

In our presented schemes, the PS operation, which is a typical non-Gaussian operation, is applied to enhance the entanglement of CV entanglement swapping. In addition to the PS operation, there are also other non-Gaussian operations, such as photon addition and photon replacement, that can be applied to enhance CV entanglement [54]. In addition, the sequence of non-Gaussian operations can also be applied to enhance the entanglement of TMSS [55]. Thus, it is worth-

while to investigate more non-Gaussian operations to enhance the entanglement of CV entanglement swapping in the future.

In our schemes, entanglement enhancement is realized by performing non-Gaussian operations, which lead to the non-Gaussian states. To our knowledge, there are two methods to proceed with the next entanglement swapping by using the resulting non-Gaussian state. One is that the next entanglement swapping is implemented based on the Gaussian state. In this case, the ‘‘Gaussification’’ step is required to transform the non-Gaussian state into the approximate Gaussian state at first [56–59], and then the next entanglement swapping is implemented based on the approximate Gaussian state. The other method is that the next entanglement swapping is realized directly based on non-Gaussian resources, which warrants further investigation.

In summary, we propose a scheme of enhancing the entanglement of CV entanglement swapping by PS operations. We show that both one- and two-sided PS operations can enhance the entanglement after the entanglement swapping in lossy single- and dual-channel transmission schemes. Compared to the one-sided PS operation, the two-sided PS operation enables one to obtain higher entanglement of CV entanglement swapping, and the maximum transmission distance with PS operations of the single-channel transmission scheme is longer than that of the dual-channel transmission scheme in the lossy channel. We also show that the transmission distance where the two-sided PS operation takes effect decreases with the increase of excess noise in the noisy single-channel scheme. Our work shed light on the combination of entanglement swapping and non-Gaussian operations to enhance the entanglement in the CV entanglement swapping. The presented results have potential applications in building entanglement-based quantum repeaters by combining them with quantum memory.

ACKNOWLEDGMENTS

This work was financially supported by National Natural Science Foundation of China (Grants No. 62275145, No. 11834010), Fundamental Research Program of Shanxi Province (Grant No. 20210302121002), and the Fund for Shanxi ‘‘1331 Project’’ Key Subjects Construction.

-
- [1] M. Żukowski, A. Zeilinger, M. A. Horne, and A. K. Ekert, *Phys. Rev. Lett.* **71**, 4287 (1993).
 [2] S. M. Tan, *Phys. Rev. A* **60**, 2752 (1999).
 [3] P. van Loock and S. L. Braunstein, *Phys. Rev. A* **61**, 010302(R) (1999).
 [4] V. N. Gorbachev, A. I. Zhiliba, and A. I. Trubilko, *J. Opt. B* **3**, S25 (2001).
 [5] J.-W. Pan, D. Bouwmeester, H. Weinfurter, and A. Zeilinger, *Phys. Rev. Lett.* **80**, 3891 (1998).
 [6] X. Jia, X. Su, Q. Pan, J. Gao, C. Xie, and K. Peng, *Phys. Rev. Lett.* **93**, 250503 (2004).
 [7] N. Takei, H. Yonezawa, T. Aoki, and A. Furusawa, *Phys. Rev. Lett.* **94**, 220502 (2005).
 [8] X. Su, C. Tian, X. Deng, Q. Li, C. Xie, and K. Peng, *Phys. Rev. Lett.* **117**, 240503 (2016).
 [9] S. Takeda, M. Fuwa, P. van Loock, and A. Furusawa, *Phys. Rev. Lett.* **114**, 100501 (2015).
 [10] G. Guccione, T. Darras, H. Le Jeannic, V. B. Verma, S. Woo Nam, A. Cavaillés, and J. Laurat, *Sci. Adv.* **6**, eaba4508 (2020).
 [11] W. H. Zurek, *Rev. Mod. Phys.* **75**, 715 (2003).
 [12] T. Yu, and J. H. Eberly, *Science* **323**, 598 (2009).
 [13] M. P. Almeida, F. de Melo, M. Hor-Meyll, A. Salles, S. P. Walborn, P. H. Souto Ribeiro, and L. Davidovich, *Science* **316**, 579 (2007).
 [14] J. Eisert, S. Scheel, and M. B. Plenio, *Phys. Rev. Lett.* **89**, 137903 (2002).

- [15] J. Fiurášek, *Phys. Rev. Lett.* **89**, 137904 (2002).
- [16] G. Giedke and J. I. Cirac, *Phys. Rev. A* **66**, 032316 (2002).
- [17] A. Kitagawa, M. Takeoka, M. Sasaki, and A. Chefles, *Phys. Rev. A* **73**, 042310 (2006).
- [18] S. L. Zhang and P. van Loock, *Phys. Rev. A* **82**, 062316 (2010).
- [19] C. Navarrete-Benlloch, R. García-Patrón, J. H. Shapiro, and N. J. Cerf, *Phys. Rev. A* **86**, 012328 (2012).
- [20] T. J. Bartley, P. J. D. Crowley, A. Datta, J. Nunn, L. Zhang, and I. Walmsley, *Phys. Rev. A* **87**, 022313 (2013).
- [21] S. Y. Lee, S. W. Ji, and C. W. Lee, *Phys. Rev. A* **87**, 052321 (2013).
- [22] P. Zhang, H. R. Li, H. Gao, and F. L. Li, *J. Mod. Opt.* **58**, 835 (2011).
- [23] S. L. Zhang, Y. L. Dong, X. B. Zou, B. S. Shi, and G. C. Guo, *Phys. Rev. A* **88**, 032324 (2013).
- [24] S. Y. Lee, S. W. Ji, H. J. Kim, and H. Nha, *Phys. Rev. A* **84**, 012302 (2011).
- [25] J. Lee and H. Nha, *Phys. Rev. A* **87**, 032307 (2013).
- [26] Y. Mardani, A. Shafiei, M. Ghadimi, and M. Abdi, *Phys. Rev. A* **102**, 012407 (2020).
- [27] T. Opatrný, G. Kurizki, and D. G. Welsch, *Phys. Rev. A* **61**, 032302 (2000).
- [28] F. Dell'Anno, S. De Siena, L. Albano, and F. Illuminati, *Phys. Rev. A* **76**, 022301 (2007).
- [29] F. Dell'Anno, S. De Siena, and F. Illuminati, *Phys. Rev. A* **81**, 012333 (2010).
- [30] P. Huang, G. He, J. Fang, and G. Zeng, *Phys. Rev. A* **87**, 012317 (2013).
- [31] H. X. Ma, P. Huang, D. Y. Bai, S. Y. Wang, W. S. Bao, and G. H. Zeng, *Phys. Rev. A* **97**, 042329 (2018).
- [32] Y. Guo, W. Ye, H. Zhong, and Q. Liao, *Phys. Rev. A* **99**, 032327 (2019).
- [33] R. Birrittella, J. Mimih, and C. C. Gerry, *Phys. Rev. A* **86**, 063828 (2012).
- [34] R. Carranza and C. C. Gerry, *J. Opt. Soc. Am. B* **29**, 2581 (2012).
- [35] D. Braun, P. Jian, O. Pinel, and N. Treps, *Phys. Rev. A* **90**, 013821 (2014).
- [36] U. L. Andersen, J. S. Neergaard-Nielsen, P. Van Loock, and A. Furusawa, *Nat. Phys.* **11**, 713 (2015).
- [37] P. van Loock, *Laser Photon. Rev.* **5**, 167 (2011).
- [38] S. Ren, Y. Wang, and X. Su, *Sci. China Inf. Sci.* **65**, 200502 (2022).
- [39] F. Dell'Anno, D. Buono, G. Nocerino, S. De Siena, and F. Illuminati, *Quant. Inf. Proc.* **18**, 20 (2019).
- [40] C. Weedbrook, S. Pirandola, R. García-Patrón, N. J. Cerf, T. C. Ralph, J. H. Shapiro, and S. Lloyd, *Rev. Mod. Phys.* **84**, 621 (2012).
- [41] P. van Loock, *Fortschr. Phys.* **50**, 1177 (2002).
- [42] J. Hoelscher-Obermaier and P. van Loock, *Phys. Rev. A* **83**, 012319 (2011).
- [43] G. Vidal and R. F. Werner, *Phys. Rev. A* **65**, 032314 (2002).
- [44] M. B. Plenio, *Phys. Rev. Lett.* **95**, 090503 (2005).
- [45] A. I. Lvovsky and M. G. Raymer, *Rev. Mod. Phys.* **81**, 299 (2009).
- [46] A. Ourjoumtsev, R. Tualle-Brouiri, and P. Grangier, *Phys. Rev. Lett.* **96**, 213601 (2006).
- [47] M. Cooper, L. J. Wright, C. Söller, and B. J. Smith, *Opt. Express* **21**, 5309 (2013).
- [48] M. Wang, M. Zhang, Z. Qin, Q. Zhang, L. Zeng, X. Su, C. Xie, and K. Peng, *Laser Photon. Rev.* **16**, 2200336 (2022).
- [49] D. Han, F. Sun, N. Wang, Y. Xiang, M. Wang, M. Tian, Q. He, and X. Su, *Laser Photon. Rev.* **17**, 2300103 (2023).
- [50] S. Liu, D. Han, N. Wang, Y. Xiang, F. Sun, M. Wang, Z. Qin, Q. Gong, X. Su, and Q. He, *Phys. Rev. Lett.* **128**, 200401 (2022).
- [51] Y. Kurochkin, A. S. Prasad, and A. I. Lvovsky, *Phys. Rev. Lett.* **112**, 070402 (2014).
- [52] H. Takahashi, J. Neergaard-Nielsen, M. Takeuchi, M. Takeoka, K. Hayasaka, A. Furusawa, and M. Sasaki, *Nat. Photon.* **4**, 178 (2010).
- [53] A. E. Ulanov, I. A. Fedorov, A. A. Pushkina, Y. V. Kurochkin, T. C. Ralph, and A. I. Lvovsky, *Nat. Photon.* **9**, 764 (2015).
- [54] T. J. Bartley and I. A. Walmsley, *New J. Phys.* **17**, 023038 (2015).
- [55] E. Villaseñor and R. Malaney, in *Proceedings of the IEEE Global Commun. Conference, Madrid, 2021* (IEEE, Piscataway, NJ, 2021), pp. 1–6.
- [56] D. E. Browne, J. Eisert, S. Scheel, and M. B. Plenio, *Phys. Rev. A* **67**, 062320 (2003).
- [57] J. Eisert, D. E. Browne, S. Scheel, and M. B. Plenio, *Ann. Phys.* **311**, 431 (2004).
- [58] E. T. Campbell and J. Eisert, *Phys. Rev. Lett.* **108**, 020501 (2012).
- [59] E. T. Campbell, M. G. Genoni, and J. Eisert, *Phys. Rev. A* **87**, 042330 (2013).